

## Infrared reflectance spectra of the sodium tungsten bronzes: evidence for a surface depletion layer

This article has been downloaded from IOPscience. Please scroll down to see the full text article.

1989 J. Phys.: Condens. Matter 1 SB123

(<http://iopscience.iop.org/0953-8984/1/SB/021>)

View [the table of contents for this issue](#), or go to the [journal homepage](#) for more

Download details:

IP Address: 129.252.86.83

The article was downloaded on 27/05/2010 at 11:11

Please note that [terms and conditions apply](#).

## Infrared reflectance spectra of the sodium tungsten bronzes: evidence for a surface depletion layer

J P Kemp<sup>†</sup>, P A Cox<sup>†</sup>, R G Egdell<sup>‡</sup> and K Kang<sup>‡</sup>

<sup>†</sup> Inorganic Chemistry Laboratory, South Parks Road, Oxford OX1 3QR, UK

<sup>‡</sup> Department of Chemistry, Imperial College, London SW7 2AZ, UK

Received 14 April 1989

**Abstract.** Infrared reflectance spectra of (001) surfaces of the sodium tungsten bronzes  $\text{Na}_x\text{WO}_3$  have been measured in air. Reflectance minima are found close to the highest bulk LO phonon frequency. Comparison with model calculations suggests that there is a depletion layer 10 Å thick on the bronze surface.

### 1. Introduction

Conduction electrons in metallic oxides such as the sodium tungsten bronzes  $\text{Na}_x\text{WO}_3$  screen out coupling between phonon modes of the oxide lattice and external electromagnetic fields. However, the screening may not be perfect close to the surface owing to the non-vanishing screening length and the possibility that there may be surface depletion layers. We have previously shown that the main features of the high resolution electron energy-loss spectra of the tungsten bronzes in the region of vibrational losses may be accounted for by introducing the screening length explicitly, either via a two-layer model [1], or a hydrodynamic model with appropriate surface boundary conditions [2–4]. In this work we employ a similar approach to attempt both to rationalise the appearance of infrared reflectance spectra of these systems and to investigate whether the range of validity of either model extends to techniques other than EELS.

### 2. Experimental details

Crystals of  $\text{Na}_x\text{WO}_3$  with (001) surfaces up to 1 cm<sup>2</sup> were prepared by electrolytic reduction of molten  $\text{Na}_2\text{WO}_4/\text{WO}_3$  mixtures at a Ta cathode. The growth surfaces were polished with successively finer diamond pastes down to 1 μm and then ultrasonically rinsed in isopropanol. Reflectance spectra were measured at a 45° angle of incidence with unpolarised radiation using a Mattson Alpha Centauri interferometer equipped with a KBr beam splitter and DTGS detector. Reflectance was ratioed against an Al mirror. The spectrum of the purple bronze with  $x = 0.6$  is shown in figure 1. Note the sharp reflectivity dip at 680 cm<sup>-1</sup>, together with a broader dip centred at 940 cm<sup>-1</sup>. These values fall close to estimated bulk TO (766 cm<sup>-1</sup>) and LO (967 cm<sup>-1</sup>) phonon frequencies for the W–O stretching modes of the host cubic  $\text{WO}_3$  framework.

### 3. Theoretical modelling

A general theory of surface response to electromagnetic fields has been advanced by García-Moliner and Flores [5, 6]. They define a surface impedance tensor  $\mathbf{Z}$  as follows:

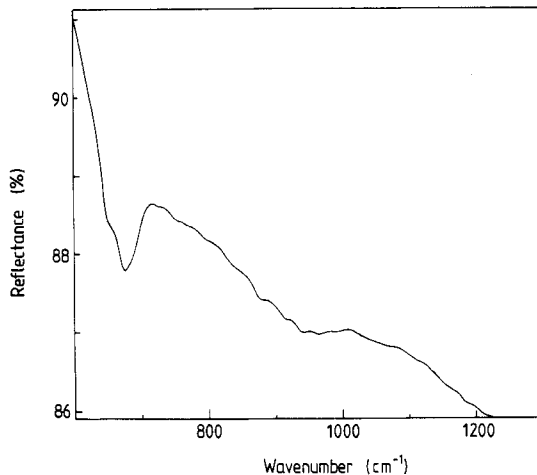


**Figure 1.** The IR reflectance spectrum of  $\text{Na}_{0.6}\text{WO}_3$  measured at  $16\text{ cm}^{-1}$  resolution in the region between  $600$  and  $1200\text{ cm}^{-1}$ .

$$\mathbf{E}_{\parallel}^{\S} = (c/4\pi)\mathbf{Z}(\mathbf{n} \times \mathbf{H}^{\S}) \quad (1)$$

where  $c$  is the speed of light,  $\mathbf{n}$  the unit outer normal from the surface,  $\mathbf{H}^{\S}$  the magnetic field at the surface and  $\mathbf{E}_{\parallel}^{\S}$  the electric field parallel to the surface, evaluated at the surface. For p-mode radiation ( $\mathbf{H}$  parallel to the surface) and if two media are assumed to occupy the two halves of space  $z > 0$  and  $z < 0$ , the surface impedances are

$$\begin{aligned} Z_p^{\>} &= + (4\pi/c)(E_x/H_y)_{z \rightarrow +0} & \text{for } z > 0 \\ Z_p^{\<} &= - (4\pi/c)(E_x/H_y)_{z \rightarrow -0} & \text{for } z < 0. \end{aligned} \quad (2)$$

On applying matching conditions on  $\mathbf{E}$  and  $\mathbf{H}$  across the interface, incident and reflected amplitudes are found to be related via

$$H_{y,\text{ref}}(z \rightarrow -0)/H_{y,\text{inc}}(z \rightarrow -0) = (Z_p^{\<} + Z_p^{\>})/(Z_p^{\<} - Z_p^{\>}) \quad (3)$$

For a vacuum in  $z < 0$  and radiation incident at  $\theta_i$ ,

$$Z_p^{\<} = - (4\pi/c) \cos \theta_i \quad (4)$$

and the ratio of reflected and incident intensities becomes:

$$R = |[Z_p^{\>} - (4\pi/c) \cos \theta_i]/[Z_p^{\>} + (4\pi/c) \cos \theta_i]|^2. \quad (5)$$

The surface response, as given by  $Z_p$ , is found by solution of Maxwell's equations [5–7] (in cgs units) to be

$$Z_p^{\>} = - \frac{1}{\pi} \int_{z \rightarrow 0} \exp(iqz) G_{xx}(\mathbf{k}) dq \quad (6)$$

where  $G_{xx}$  is a component of the tensor

$$\mathbf{G}(\mathbf{k}, \omega) = \frac{4\pi i}{\omega} \left( - \frac{\mathbf{k}\mathbf{k}}{k^2 \epsilon_l} + \frac{\omega^2}{c^2} \frac{(k^2 \mathbf{l} - \mathbf{k}\mathbf{k})}{k^2(k^2 - \epsilon_t \omega^2/c^2)} \right) \quad (7)$$

with  $\epsilon_l$  and  $\epsilon_t$  the longitudinal and transverse dielectric functions,  $\mathbf{l}$  the unit tensor and  $\mathbf{k}\mathbf{k}$  the tensor whose  $(i, j)$  component is  $k_i k_j$  and, in p-mode, the wavevector  $\mathbf{k}$  has components  $(\kappa, 0, q)$ . There have, however, been few attempts to use the above framework to model the effects of surface screening in reflectance spectra. To evaluate the reflectivity from (5) requires a model dielectric function  $\epsilon(\mathbf{k}, \omega)$  for (7) and thence (6). One that allows the integration to be performed analytically is the hydrodynamic function:

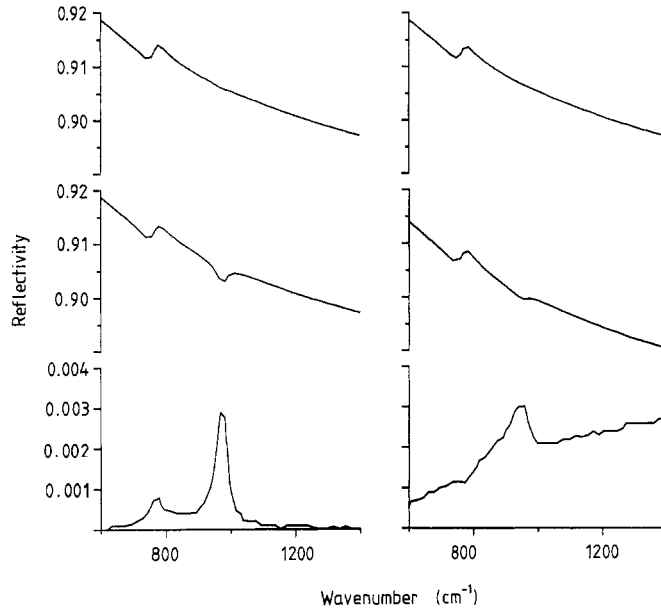


**Figure 2.** Calculated reflectance spectra for  $\text{Na}_{0.6}\text{WO}_3$  obtained using the two-layer model (left-hand group) and the hydrodynamic model (right-hand group). The screening lengths are 1.2 Å (upper pair) and 10 Å (centre). The lower pair shows the difference between the centre pair and perfect screening.

$$\varepsilon(\mathbf{k}, \omega) = \varepsilon_{\infty} + \varepsilon_{\text{vib}} - \varepsilon_{\infty} \Omega_{\text{p}}^2 / (\omega^2 - \beta^2 k^2 + i\omega/\tau) \quad (8)$$

where the dispersion parameter  $\beta$ , by identity with the Lindhardt function [8], may be related to the effective mass and Fermi wavevector for the system, and is directly proportional to the screening length [2].

The ‘two-layer’ model may also be used. This assumes that there is a carrier-free surface layer, whose thickness may be equated with the screening length if the bands are flat. However, band bending may produce surface depletion layers with a thickness greater than the screening length. In this model, it is necessary to consider two interfaces (vacuum/depletion and depletion layer/bulk). The relevant surface impedances are given by (6) and (7) and the damping of the electromagnetic waves across the depletion layer (due to absorption) may be found from a generalisation of (6) [6]. Matching conditions applied to the incident, reflected and transmitted waves at each interface allow the reflectivity to be given by an expression analogous to (5), but with an effective surface impedance of

$$Z'_{\text{p}} = Z_{\text{d}}(1 + D^2 R') / (1 - D^2 R'). \quad (9)$$

Here  $Z_{\text{d}}$  is the depletion layer impedance,  $Z_{\text{m}}$  the bulk (metal) impedance,  $R' = (Z_{\text{m}} - Z_{\text{d}}) / (Z_{\text{m}} + Z_{\text{d}})$  and  $D$  is the damping factor, given by

$$D = \exp(-|\text{Im}(\varepsilon_{\text{d}} \omega^2 / c^2 - \kappa^2)|d) \quad (10)$$

for a depletion layer thickness  $d$  and dielectric function  $\varepsilon_{\text{d}}$ . Note that as  $d \rightarrow 0$ ,  $D \rightarrow 1$  and  $Z'_{\text{p}} \rightarrow Z_{\text{m}}$  and that as  $d \rightarrow \infty$ ,  $D \rightarrow 0$  and  $Z'_{\text{p}} \rightarrow Z_{\text{d}}$ , as expected. The formulae also bear a strong formal resemblance to those derived for the two-layer model in its application to EELS [9].

Figure 2 shows reflectance spectra calculated for unpolarised (i.e. mixed s- and p-mode) radiation incident at  $45^\circ$  to a  $\text{Na}_{0.6}\text{WO}_3$  surface for two values of the relevant length parameter, using both models. (The dielectric data were the same as those used in previous studies [1, 2].) The upper pair of spectra show those for a length of  $1.2 \text{ \AA}$ , the action screening length. No dip in the reflectivity is discernible in the region of the LO phonon,  $900\text{--}1000 \text{ cm}^{-1}$ , although there is a pronounced dip around  $750 \text{ cm}^{-1}$ . As the length parameter is increased, a dip develops around  $950 \text{ cm}^{-1}$  and for large values the spectra evolve into the typical restrahl (i.e. with a strong reflectance maximum between  $\omega_{\text{TO}}$  and  $\omega_{\text{LO}}$ ) spectra expected for a polar insulator.

The centre spectra show the best fit to the experimental spectrum. Agreement is very good, in terms of the absolute reflected intensity, and the intensities of the reflectance minima at  $\omega_{\text{TO}}$  and  $\omega_{\text{LO}}$ , especially for the hydrodynamic model. Both, however, correspond to a length parameter in the region of  $10 \text{ \AA}$ , rather greater than the true screening length (which gives good agreement with observed EEL spectra [2]). However, the EEL spectra were recorded from a vacuum-annealed crystal, while in this work measurements were performed in air, and it is quite possible that we are seeing the effects of oxidative carrier depletion. More specifically, if chemisorption of oxygen to yield a monolayer of  $\text{O}^{2-}$  is assumed, this would deplete the carriers from three unit cells per adsorbed atom, giving rise to a depletion layer of the same depth as that in the calculations. Further work is clearly needed, though, to place these conclusions on a more concrete footing, and we are currently extending our measurements to ultra-high-vacuum conditions, where surface stoichiometry can be more closely controlled and monitored.

The lowest pair of spectra in figure 2 show the difference between spectra calculated for perfect screening, and those above. An interesting difference here is that the two-layer model concentrates the spectral weight into a single sharp line, whereas that in the hydrodynamic model is spread out into a tail extending towards the TO phonon frequency, in a similar manner to what is observed experimentally. This effect has been previously discussed [2] in relation to the EEL spectra of this compound, and so we shall not dwell further on it here.

In conclusion, we have demonstrated that use of relatively simple models for surface response incorporating the screening length and depletion layers explicitly allows a quantitative interpretation of IR reflectance spectra of polar metals, both in terms of intensities of features observed, and, for the hydrodynamic model, lineshapes, given reasonable assumptions concerning surface composition. It therefore has the potential to provide a means whereby useful surface chemical information may be obtained, e.g. on surface screening, outside of a UHV environment.

## References

- [1] Cox P A, Hill M D, Peplinski F and Egdell R G 1984 *Surf. Sci.* **141** 13
- [2] Cox P A and Kemp J P 1989 *Surf. Sci.* **210** 225
- [3] Inaoka T, Newns D M and Egdell R G 1987 *Surf. Sci.* **186** 290
- [4] Schaich W L 1982 *Surf. Sci.* **122** 175
- [5] García-Moliner F and Flores F 1977 *J. Physique* **38** 851
- [6] Flores F and García-Moliner F 1979 *Introduction to the Theory of Solid Surfaces* (Cambridge: CUP)
- [7] Ritchie R H and Maruzak A L 1966 *Surf. Sci.* **4** 234
- [8] Pines D and Nozières P 1966 *The Theory of Quantum Liquids* vol 1 (New York: Benjamin)
- [9] Ibach H and Mills D L 1982 *Electron Energy Loss Spectroscopy and Surface Vibrations* (New York: Academic)